Performance of MgO:PPLN, KTA and $KNbO_3$ for mid-wave infrared broadband parametric amplification at high average power

M. Baudisch[1*], M. Hemmer[1], H. Pires[1], J. Biegert[1,2]

[1]*ICFO - Institut de Ciencies Fotoniques, Mediterranean Technology Park, Castelldefels, Spain.*
[2]*ICREA - Institució Catalana de Recerca i Estudis Avançats, Barcelona, Spain.*
**Corresponding author: matthias.baudisch@icfo.eu*

The performance of $KNbO_3$, MgO:PPLN and KTA were experimentally compared for broadband mid-wave infrared parametric amplification at high repetition rate. The seed pulses with an energy of 6.5 µJ were amplified using 410 µJ of pump at 1064 nm to a maximum pulse energy of 28.9 µJ at 3 µm wavelength and at 160 kHz repetition rate in MgO:PPLN while supporting a transform limited duration of 73 fs. The high average powers of the interacting beams used in this study, revealed average power induced processes which limit the scaling of optical parametric amplification: in MgO:PPLN the pump peak intensity was limited to 3.8 GW/cm^2 due to non-permanent beam reshaping while in $KNbO_3$ an absorption-induced temperature gradient in the crystal led to permanent internal distortions in the crystal structure when operated above a pump peak intensity of 14.4 GW/cm^2.

Mid-wave infrared (MWIR) sources, with wavelength between 3 µm and 8 µm, operating at high repetition rate and high average power are important for a wide range of applications, e.g. in medicine [1], spectroscopy [2] and strong-field physics [3]. Although there are some promising developments in laser gain material in this spectral region, such as Cr:ZnSe and Cr:ZnS [4], the amplification of high-energy broadband MWIR light typically makes use of optical parametric amplification (OPA).

Contrary to traditional laser amplifiers relying on storage of the pump power, parametric amplifiers are often claimed to be free of thermal loading due to the instantaneous nature of the nonlinear interaction. It has nonetheless recently been shown in a near-IR BBO-based OPA [5] that residual absorption of the interacting waves can lead to considerable thermal loading of the gain medium when operated at high average power. Such loading sets an upper-bound to the scalability of OPAs and optical parametric chirped-pulse amplification (OPCPA) systems as it leads to the common adverse effects observed in gain storage amplifiers and additionally modifies the phase-matching conditions for broadband amplification.

Various pulsed mid-IR OPAs supporting pulse durations in the fs regime have been reported. At 1 kHz OPAs featuring various materials, such as GaSe [6], $KNbO_3$ [7], KTP [7], KTA [7], MgO:PPLN [8] and PPSLT [9] where demonstrated with pulse energies in the mid-IR idler up to 550 µJ corresponding to an average power of 550 mW. At tens of kHz repetition rates mid-IR OPAs reaching at least nJ level of energy were demonstrated in KTP [10], in bulk $LiNbO_3$ [11] and MgO:PPLN [12]. The maximum amplified idler average power was 600 mW.

In this paper we investigate the suitability of Potassium Niobate ($KNbO_3$), MgO-doped periodically-poled Lithium Niobate (MgO:PPLN) and Potassium Titanyl Arsenate (KTA) for broadband MWIR parametric amplification at high average pump power. The potential of these crystals for energy scaling of ultra-broadband optical pulses in the MWIR spectral range to the multi-tens of microjoule energy level at 160 kHz repetition rate – corresponding to the 1-10 W average power level – is demonstrated. The intrinsic crystal limitations encountered for each crystal are detailed and discussed.

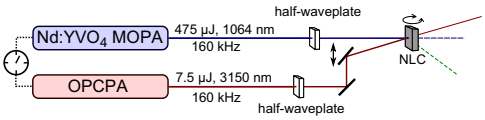

Fig. 1. Schematic of the experimental test-bed used for investigating the potential of $KNbO_3$, MgO:PPLN and KTA as OPA gain media at high average pump power. The setup is highly versatile, enabling tuning of all relevant parameters (NLC: non linear crystal).

The MWIR source used in this study delivered 3.5 ps duration temporally stretched optical pulses exhibiting 390 nm of spectral bandwidth (1/e^2 width) at 3.15 µm central wavelength at 160 kHz repetition rate. It shares the same front-end as the OPCPA system described in [13]. The pump laser was a commercial Nd:YVO_4-based master oscillator power amplifier system (Coherent GmbH) delivering up to 475 µJ energy pulses at 160 kHz with a temporal duration of 9.5 ps in a Gaussian spatial intensity profile. The pump laser was electronically synchronized to the MWIR source via locking of the repetition rates with a commercial synchronization unit

Table 1: Comparison of nonlinear crystals suitable for parametric amplification of MWIR radiation between 2.5 and 4 µm. Transparency ranges, best phase-matching angles, noncollinear angles and the effective second-order nonlinear coefficients d_{eff} are obtained from SNLO [14]. The parametric phase-matching (PM) bandwidths were computed for a crystal length $L = 2$ mm at a center

Formatted: Spanish

Deleted: Received Month X, XXXX; revised Month X, XXXX; accepted Month X, XXXX; posted Month X, XXXX (Doc. ID XXXXX); published Month X, XXXX

Deleted: © 2014 Optical Society of America ... [1]

wavelength λ = 3.15 µm (calculated according to Eqn. 11 in [15]). The damage threshold for PPLT is taken from [16] and for all other crystals from [17].

	Transp. range (µm)	PM angle / QPM-period, PM type	Noncoll. angle (degrees)	d_{eff} (pm/V)	PM bandwidth (nm) at 3.15 µm	Damage threshold @ 1064 nm (GW/cm²)
Bulk materials						
MgO-doped Lithium Niobate (MgO:LN)	0.33 - 5.5	48.0°, type I	5.7	-4.0	456 nm	10 (6 ps)
Lithium Iodate (LIO)	0.3 - 6.0	20.3°, type I	3.2	1.3	790 nm	19 (45 ps)
Potassium Niobate ($KNbO_3$)	0.4 - 4.5	40.3°, type I	5.0	6.0	486 nm	100 (100 ps)
Potassium Titanyl Arsenate (KTA)	0.35 - 4.0	42.1°, type II	0	-2.1	222 nm	>1.2 (8 ns)
Potassium Titanyl Phosphate (KTP)	0.35 - 4.5	46.1°, type II	0	-2.3	266 nm	15 (1 ns)
Periodically poled materials						
Lithium Tantalate (PPLT)	0.28 - 5.5	31.0 µm	0	10.4	195 nm	>80 (30 ps)
MgO-doped Lithium Niobate (MgO:PPLN)	0.33 - 5.5	31.0 µm	0	14.8	233 nm	10 (6 ps)

(Toptica Photonics AG). The setup, shown in Fig. 1, permitted changing the spatio-temporal overlap of pump and seed signals for collinear, non-collinear, type I or type II interactions; all crystals were mounted without active cooling. In the case of collinear interaction custom-made dielectric coated filters were placed in the output beam to separate pump, idler and signal beams, ensuring unambiguous measurement of the amplified energy. MWIR spectra were measured using a Fourier transform infrared (FTIR, Oriel Instruments) spectrometer equipped with a liquid nitrogen cooled HgCdTe (MCT) detector which was wavelength and intensity calibrated.

The choice of the nonlinear crystals satisfying the aim for ultra-broadband parametric amplification was limited to the few oxyde crystals – either bulk or periodically poled – exhibiting transparency in the MWIR (Table 1). The choice of the material amongst those listed in Table 1 was dictated by the aim of obtaining the highest output energy simultaneously with the widest amplified spectral bandwith. $KNbO_3$ was chosen as it exhibits the highest effective nonlinear coefficient (d_{eff}) for bulk materials, high reported damage threshold and a wide phase-matchable bandwidth exceeding the spectral extent of the seed pulses. As a drawback it requires resorting to non-collinear interaction, potentially resulting in spatial profile distortions. KTA was chosen as it enables simple collinear amplification. While KTP appears to offer a higher d_{eff} and wider phase-matchable bandwidth than KTA, the absorption coefficient of KTA in the spectral range 3.0-3.5 µm is at least an order of magnitude smaller than that of KTP [18]. Periodically poled materials offer the highest effective nonlinear coefficient and therefore the best prospects for high energy amplification. Nonetheless, the very nature of the periodic poling reduces the amplifiable bandwidth and might result in parasitic phase-matching. For this study we chose MgO:PPLN over PPLT since it exhibits both a wider phase-matchable bandwidth and a larger d_{eff}.

Based on these considerations, three crystals with comparable length were selected: (i) a 1.8 mm long $KNbO_3$ crystal cut at 40.5°, (ii) a large aperture (5x5 mm²) 2.18 mm long MgO:PPLN crystal with a quasi-phase-matching QPM period of 31.0 µm [19] and (iii) a 2.0 mm long KTA crystal cut at 41.7°. Experimentally, each crystal was placed under optimal phase-matching conditions to ensure the broadest amplification bandwidth. The pump beam size was adjusted for stable operation at the maximum available pump power slightly below the damage threshold (Table 1) or below the threshold for any other observable parasitic effect altering the amplified output. The seed beam size was matched to that of the pump.

The spectral behavior of each crystal was investigated first and the results are presented in Fig. 2. The spectra shown were recorded at the highest possible seed amplification level. As expected from preliminary calculations (Table 1), $KNbO_3$ features an output spectrum similar to the input spectrum. The 1/e² bandwidth of 370 nm supports a transform limit of 73 fs, potentially yielding amplified 7-cycle duration optical

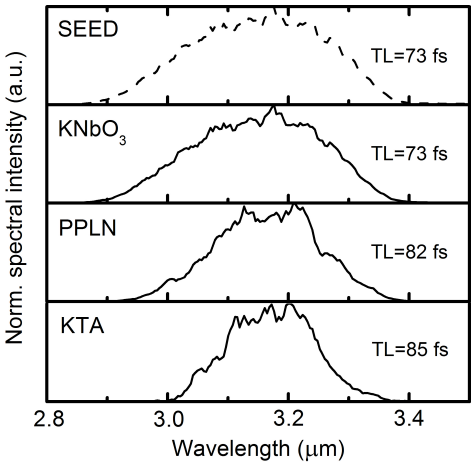

Fig. 2. From top to bottom: measured input seed spectrum and amplified spectrum at maximum pump intensity for $KNbO_3$, PPLN and KTA.

pulses. The 1/e² spectral width amplified in MgO:PPLN was 350 nm and yielded a transform limit of 82.3 fs, representing a 13.8% increase in duration compared to

the seed pulse. The amplified spectrum in KTA is relatively narrow compared to the input spectrum. It exhibits a $1/e^2$ bandwidth of 320 nm corresponding to transform limited pulse durations of 85 fs, representing a 16.5% increase in transform limited pulse duration during the amplification process.

The potential of each crystal as an amplifier medium was then investigated and the results are presented in Fig. 3. The pump and seed beam waists ($1/e^2$ radius) were set to 436 µm, 852 µm, and 214 µm for $KNbO_3$, MgO:PPLN and KTA respectively to operate close to the reported damage threshold (for KTA) or limiting parasitic process threshold (for $KNbO_3$ and MgO:PPLN). At the maximum available pump pulse energy amplification up to 28.6 µJ was achieved in $KNbO_3$, 28.9 µJ in MgO:PPLN and 26.8 µJ in KTA.

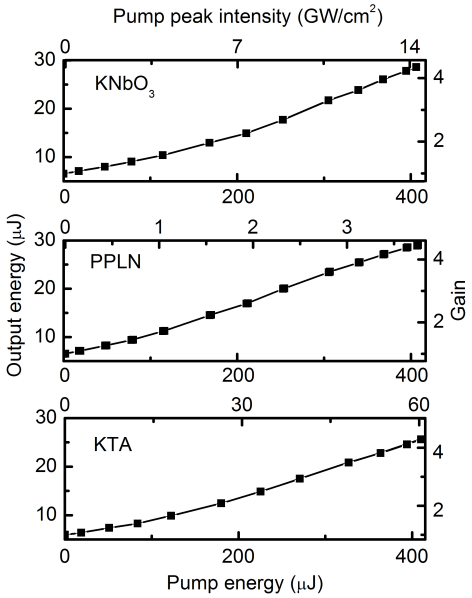

Fig. 3. Measured amplified MWIR output pulse energy versus pump pulse energy (bottom abscissa axis) and pump peak intensity (top abscissa axis). The measured matched pump and signal waists were set to $w = 436$ µm for $KNbO_3$, $w = 852$ µm for PPLN, and $w = 214$ µm for KTA. The data are corrected to account for Fresnel reflections.

All crystals provided comparable performance and exhibited a gain of ~4.4 and a total conversion efficiency of the pump wave to the signal plus idler waves of 16.3% for KNbO3, 16.5% for PPLN and 14.4% for KTA. The linear shape of the power scaling curve (Fig. 3) indicates that the amplifier was operated away from the depletion regime and that higher energy extraction could be achieved. In the case of our experiment, and without resorting to any spatio-temporal shaping, this would require resorting to longer crystals at the expense of bandwidth.

The crystal-specific processes limiting energy scaling were then investigated. In the case of $KNbO_3$, intensities of 14.4 GW/cm² could not be exceeded, a value well below the 100 GW/cm² reported in the literature (Table 1) for 100 ps pump duration. Even the empirical square root scaling for the damage threshold predicts a factor two higher threshold than observed. For intensities higher than 14.4 GW/cm², we observed the formation of distinct lines, which were visible to the naked-eye, within the crystal that could partially be removed by carefully sintering the crystal after usage (Fig. 4). Formation of such lines has previously been reported [20, 21] as differently oriented domains in the ferroelectric material $KNbO_3$. At room temperature the crystal is in an orthorhombic structure and a formation of a domain pattern, especially at defects in the crystal structure, can occur close to the phase transition temperature (~220°C) [20] or at lower temperatures via steep temperature gradients or pressure gradients [21]. In our experiment such temperature gradient was possibly induced by localized heating – inherent to the high average power of high repetition rate systems – induced by the residual absorption of the pump and the amplified seed beam in the crystal ultimately limiting the achievable peak intensity and amplification. Note that great care was taken during the experiment to slowly increase the pump power, at a rate less than 1 Watt per second, to avoid thermally shocking the crystal.

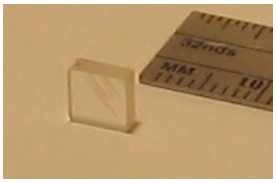

Fig. 4. Photograph of visible domain inversions (appearing as diagonal straight lines) in a $KNbO_3$ crystal after exposure to excessive thermal stress.

In KTA, no limitations were observed and we could focus the pump beam to intensities as high as 63.5 GW/cm² without inducing any damages. The peak intensity was not further increased since the reported damage threshold was already exceeded and normal antireflection coatings would probably not withstand such high peak intensities.
In the case of MgO:PPLN dramatic beam distortions were observed for intensities exceeding 3.8 GW/cm² (Fig. 5), a value less than half the damage threshold of 10 GW/cm² reported in the literature (Table 1). The beam profile of the pump was measured with a CCD camera placed 75 cm after the crystal. While increasing the pulse energy, first a slight decrease of the transmitted beam radius is observed, then symmetric ring structures around the centre of the beam appear, finally an increasing amount of pulse energy is transferred to these diffraction features. These distortions are generated by the pump beam but also affect the spatial profile of the amplified MWIR beam and the second harmonic of the pump beam which is parasitically generated due to high order QPM. Note that no damage was observed in the crystal and after reducing

the intensity below 3.8 GW/cm², the original beam profile was restored.

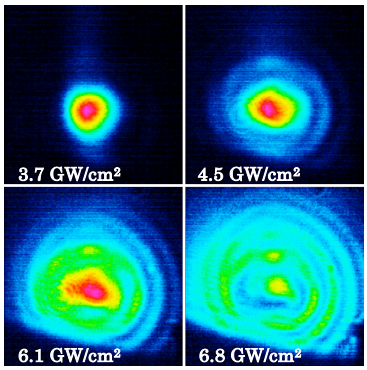

Fig. 5. Measured spatial profiles of the pump beam transmitted through the 2.18 mm thick MgO:PPLN crystal for pump peak intensities of 3.7 GW/cm² (top left), 4.5 GW/cm² (top right), 6.1 GW/cm² (bottom left) and 6.8 GW/cm² (bottom right) measured 75 cm after the crystal. The clipping observed for the highest intensities is due to size limitations on the optics directing the beam to the CCD camera.

We performed further studies of the beam reshaping process in order to get a deeper insight into the underlying physical causes. Improving our understanding of the limitations in MgO:PPLN is of particular interest, since currently all of the high average power, high repetition rate 3 µm OPCPA systems use this crystal [12, 13]. For the following discussion we will only consider the influence of the pump and its second harmonic, neglecting the effect of the idler and signal beams.

First, the applied average power was reduced by a factor of 4 while the beam was focused to a smaller size. This allowed the peak intensity to be increased to 26.7 GW/cm² without any visible beam distortion, suggesting that similar to the $KNbO_3$ case, an average power related limitation exists. Furthermore the spectrum of the distorted beam was analyzed with both a silicon-based spectrometer and a Fourier Transform Infrared Spectrometer in the spectral range from 200 nm to 2500 nm. No broadening or additional generated wavelengths were detected. This rules out Brillouin or Raman Scattering and Kerr-focusing contributions since these phenomena are accompanied by the generation of spectral side peaks and broadening respectively. In order to investigate whether the beam distortion was related to the periodic poling, we tested an unpoled bulk crystal. The latter exhibits a length of 2.00 mm, the same MgO dopant concentration of 5% and a cut angle of θ = 47°. For the same beam conditions as above no beam distortions could be observed in this unpoled crystal. This indicates that the beam reshaping process is linked to the periodic poling itself or to the stronger second harmonic generated in the periodically poled crystal.

A possible average power linked process causing the beam distortions is thermal lensing induced by linear residual absorption. This process could be further enhanced by the phenomena of GReen Induced InfraRed Absorption (GRIIRA) [22] driven by the second harmonic of the pump. Since this second harmonic at 532 nm is much stronger in the periodacally poled crystal, we were able to verify if strong GRIIRA takes place by performing a temperature measurement on both crystals. For different focussing conditions by applying the full pump power the MgO:PPLN as well as the MgO:LN crystal heated up by similar temperatures of 5.5 K ± 0.3 K indicating that no major additional absorption by GRIIRA in the periodically poled crystal takes place. The thermal lens caused by linear absorption of the pump beam can be estimated by [23]

$$f \approx \frac{\pi \cdot \omega^2 \cdot \kappa}{\alpha \cdot P \cdot L \cdot (\mathrm{d}n/\mathrm{d}T)}$$

including the beam waist ω, the thermal conductivity κ, the linear absorption coefficient α, the length of the crystal L and the temperature dependence of the refractive index dn/dT. For ω = 850 µm, κ = 4.6 W/(mK), α = 0.003 cm^{-1}, and $dn_e/dT = 3.85 \cdot 10^{-5}$ K^{-1} [17] the thermal lens introduced by 65 W at 1064 nm in a 2 mm long MgO:PPLN crystal is around 7 m, which is too long to have a serious influence on the transmitted pump beam profile.

Another possible cause for the observed beam distortions is the so-called photorefractive effect, which has been widely studied in lithium niobate [24]. A coupling between this effect and the observed pyroelectric properties of MgO:LN can induce a radial refractive index change due to temperature gradients [23]. Our investigation reveals that rather than a single of the effects listed above contribute to the beam degradation observed in MgO:PPLN, most likely a combination of the listed effects takes place, possibly one parasitic effect feeding each other. Further work would need to be undertaken to precisely identify the contribution from each effect.

In conclusion we compared the performance of $KNbO_3$, MgO:PPLN and KTA for broadband high average power, high repetition rate parametric amplification in the MWIR wavelength region. This is, to our knowledge, the first nonlinear crystal comparison in this spectral region at such high repetition rate and with amplified idler pulse energies of several tens of µJ, corresponding to the regime of 1-10 W. The seed pulse (6.5 µJ) could be amplified at a pump pulse energy of 410 µJ up to a maximum of 28.9 µJ in MgO:PPLN, corresponding to 4.6 W of average power. In $KNbO_3$ the entire spectrum ranging from 2.85 to 3.4 µm could be amplified, supporting a Fourier transform limit of 73 fs, whereas in MgO:PPLN and KTA the amplified $1/e^2$ bandwidth is reduced by 6% and 14% leading to a transform limit of 82 and 85 fs, respectivly.

The high applied average powers of 65 W pump and up to 4.6 W of MWIR idler in the amplification process, reveals also the existence of average power dependent limitations for parametric amplification processes. In $KNbO_3$ at pump peak intensities exceeding 14.4 GW/cm² permanent domain fractures appeared in the crystal structure. In

MgO:PPLN on the other hand at pump peak intensities above 3.8 GW/cm² temporary distortions of the transmitted beams occur, decreasing strongly the spatial quality of the amplified idler wave.

We conclude that $KNbO_3$ is an attractive nonlinear medium for operation up to 14.4 GW/cm² due to its large amplification bandwidth and high nonlinear coefficient for broadband MWIR. For higher amplification factors, KTA is preferred, but at the expense of spectral width. Scaling in average power, while maintaining bandwidth, will require more elaborate schemes which employ spatial, temporal or spectral multiplexing of pump and seed. Some examples are spectral coherent synthesis with two crystals in series in the same amplifier [13] where each crystal amplifies a part of the spectral bandwidth, or Fourier Plane Optical Parametric Amplification [25].

We acknowledge support from MINISTERIO DE ECONOMA Y COMPETITIVIDAD through Plan Nacional (FIS2011-30465-C02-01), the Catalan Agencia de Gestio d'Ajuts Universitaris i de Recerca (AGAUR) with SGR 2009-2013, Fundacio Cellex Barcelona, and funding from LASERLAB-EUROPE, grant agreement 228334.

References

1. B. Jean and T. Bende, Topics in Appl. Phys. 89, 530–565 (2003).
2. F. K. Tittel, D. Richter, and A. Fried, Topics in Appl. Phys. 89, 458–529 (2003).
3. T. Popmintchev, M. Chen, D. Popmintchev, P. Arpin, S. Brown, S. Alisauskas, G. Andriukaitis, T. Balciunas, A. D. Mücke, A. Pugzlys, A. Baltuska, B. Shim, S. E. Schrauth, A. Gaeta, C. Hernandez-Garcia, L. Plaja, A. Becker, A. Jaron-Becker, M. M. Murnane, and H. C. Kapteyn, Science 336, 1287–1291 (2012).
4. S. B. Mirov, V. V. Fedorov, D. V. Martyshkin, I. S. Moskalev, M. S. Mirov, and V. P. Gapontsev, Opt. Mater. Express **1**, 898-910 (2011)
5. J. Rothhardt, S. Demmler, S. Hädrich, T. Peschel, J. Limpert, and A. Tünnermann, Opt. Lett. 38, 763 (2013).
6. R.A. Kaindl, M. Wurm, K. Reimann, P. Hamm, A.M. Weiner, M. Woerner, J. Opt. Soc. Am. B **17**, 2086 (2000).
7. S. Cussat-Blanc, A. Ivanov, D. Lupinski, E. Freysz, Appl. Phys. B 70, S247–S252 (2000).
8. M. Gerrity, S. Brown, T. Popmintchev, M. Murnane, H. Kapteyn, and S. Backus, in *CLEO: 2014*, OSA Technical Digest (online) (Optical Society of America, 2014), paper STh4E.8.
9. D. Brida, C. Manzoni, G. Cirmi, M. Marangoni, S. Bonora, P. Villoresi, S. De Silvestri and G. Cerullo, J. Opt. **12**, 013001 (2010).
10. G. R. Holtom, R. A. Crowell, and X. S. Xie, J. Opt. Soc. Am. B **12**, 1723 (1995).
11. M. Bradler, C. Homann, and E. Riedle, Opt. Lett. **36**, 4212 (2011).
12. B. W. Mayer, C. R. Phillips, L. Gallmann, M. M. Fejer, and U. Keller, Opt. Lett. **38**, 4265-4268 (2013).
13. M. Hemmer, A. Thai, M. Baudisch, H. Ishizuki, T. Taira, and J. Biegert, Chin. Opt. Lett. 11, 013202 (2013).
14. A. V. Smith, SNLO version 6.1, nonlinear optics code available from A.V. Smith (A-S Photonics Albuquerque, N. Mex.).
15. L. Hongjun, Z. Wei, C. Guofu, W. Yishan, C. Zhao, and R.Chi, Appl. Phys. B 79, 569 (2004).
16. T. Fuji, N. Ishii, C. Y. Teisset, X. Gu, T. Metzger, A. Baltuška, N. Forget, D. Kaplan, A. Galvanauskas, F. Krausz, Opt. Lett. 31,1103 (2006).
17. V. G. Dmitriev, G. G. Gurzadyan, D. N. Nikogosyan, *Handbook of Nonlinear Optical Crystals*, (Springer, Berlin, 1999).
18. G. Hansson, H. Karlsson, S. Wang, and F. Laurell, Appl. Opt. 39, 5058 (2000).
19. H. Ishizuki and T. Taira, Opt. Lett. 30, 2918 (2005).
20. L. Xian-jie, Z. Xing-kui, and X. Xiu-ying, Chin. Phys. Lett. 13, 621 (1996).
21. M.M. Shamim and T. Ishidate, Solid State Comm. 113, 713 (2000).
22. Y. Furukawa, K. Kitamura, A. Alexandrovski, R. K. Route, M. M. Fejer, and G. Foulon, Appl. Phys. Lett. 78, 1970 (2001).
23. Judith R. Schwesyg, Matthias Falk, Chris R. Phillips, Dieter H. Jundt, Karsten Buse, and Martin M. Fejer, J. Opt. Soc. Am. B **28**, 1973-1987 (2011).
24. A. Ashkin, G. D. Boyd, J. M. Dziedzic, R. G. Smith, A. A. Ballman, A. A. Levinstein, and K. Nassau, Appl. Phys. Lett **9**, 72 (1966).
25. B. E. Schmidt, N. Thire, M. Boivin, A. Laramée, F. Poitras, G. Lebrun, T. Ozaki, H. Ibrahim, and F. Légaré, Nature Comm. 5, 3643 (2014).

Full References

1. B. Jean and T. Bende, "Mid-IR laser applications in medicine," Topics in Appl. Phys. 89, 530–565 (2003).
2. F. K. Tittel, D. Richter, and A. Fried, "Mid-Infrared Laser Applications in Spectroscopy," Topics in Appl. Phys. 89, 458–529 (2003).
3. T. Popmintchev, M. Chen, D. Popmintchev, P. Arpin, S. Brown, S. Alisauskas, G. Andriukaitis, T. Balciunas, A. D. Mücke, A. Pugzlys, A. Baltuska, B. Shim, S. E. Schrauth, A. Gaeta, C. Hernandez-Garcia, L. Plaja, A. Becker, A. Jaron-Becker, M. M. Murnane, and H. C. Kapteyn, "Bright Coherent Ultrahigh Harmonics in the keV X-ray Regime from Mid-Infrared Femtosecond Lasers," Science 336, 1287–1291 (2012).
4. J. Rothhardt, S. Demmler, S. Hädrich, T. Peschel, J. Limpert, and A. Tünnermann, "Thermal effects in high average power optical parametric amplifiers," Opt. Lett. 38, 763 (2013).
5. S. B. Mirov, V. V. Fedorov, D. V. Martyshkin, I. S. Moskalev, M. S. Mirov, and V. P. Gapontsev, "Progress in mid-IR Cr^{2+} and Fe^{2+} doped II-VI materials and lasers [Invited]," Opt. Mater. Express **1**, 898-910 (2011)
6. R.A. Kaindl, M. Wurm, K. Reimann, P. Hamm, A.M. Weiner, M. Woerner, "Generation, shaping, and characterization of intense femtosecond pulses tunable from 3 to 20 µm," J. Opt. Soc. Am. B **17**, 2086 (2000).
7. S. Cussat-Blanc, A. Ivanov, D. Lupinski, E. Freysz, "KTiOPO4, KTiOAsO4, and KNbO3 crystals for mid-infrared femtosecond optical parametric amplifiers: analysis and comparison," Appl. Phys. B 70, S247–S252 (2000).
8. M. Gerrity, S. Brown, T. Popmintchev, M. Murnane, H. Kapteyn, and S. Backus, "High Repetition Rate, mJ-Level, mid-IR OPCPA System," in *CLEO: 2014*, OSA Technical Digest (online) (Optical Society of America, 2014), paper STh4E.8.
9. D. Brida, C. Manzoni, G. Cirmi, M. Marangoni, S. Bonora, P. Villoresi, S. De Silvestri and G. Cerullo, **"**Few-optical-cycle pulses tunable from the visible to the mid-infrared by optical parametric amplifiers," J. Opt. **12**, 013001 (2010).
10. G. R. Holtom, R. A. Crowell, and X. S. Xie, "High-repetition-rate femtosecond optical parametric oscillator–amplifier system near 3 µm," J. Opt. Soc. Am. B **12**, 1723 (1995).
11. M. Bradler, C. Homann, and E. Riedle, "Mid-IR femtosecond pulse generation on the microjoule level up to 5 µm at high repetition rates," Opt. Lett. **36**, 4212 (2011).
12. B. W. Mayer, C. R. Phillips, L. Gallmann, M. M. Fejer, and U. Keller, "Sub-four-cycle laser pulses directly from a high-repetition-rate optical parametric chirped-pulse amplifier at 3.4 µm," Opt. Lett. **38**, 4265-4268 (2013).
13. M. Hemmer, A. Thai, M. Baudisch, H. Ishizuki, T. Taira, and J. Biegert, "18-µJ energy, 160-kHz repetition rate, 250-MW peak power mid-IR OPCPA," Chin. Opt. Lett. 11, 013202 (2013).
14. A. V. Smith, SNLO version 6.1, nonlinear optics code available from A.V. Smith (A-S Photonics Albuquerque, N. Mex.).
15. L. Hongjun, Z. Wei, C. Guofu, W. Yishan, C. Zhao, and R.Chi, "Investigation of spectral bandwidth of optical parametric amplification," Appl. Phys. B 79, 569 (2004).
16. T. Fuji, N. Ishii, C. Y. Teisset, X. Gu, T. Metzger, A. Baltuška, N. Forget, D. Kaplan, A. Galvanauskas, F. Krausz, "Parametric amplification of few-cycle carrier-envelope phase-stable pulses at 2.1 µm," Opt. Lett. 31, 1103 (2006).
17. V. G. Dmitriev, G. G. Gurzadyan, D. N. Nikogosyan, "Handbook of Nonlinear Optical Crystals", (Springer, Berlin, 1999).
18. G. Hansson, H. Karlsson, S. Wang, and F. Laurell, "Transmission measurements in KTP and isomorphic compounds," Appl. Opt. 39, 5058 (2000).
19. H. Ishizuki and T. Taira, "High-energy quasi-phase-matched optical parametric oscillation in a periodically poled MgO:$LiNbO_3$ device with a 5 mm*5 mm aperture," Opt. Lett. 30, 2918 (2005).
20. L. Xian-jie, Z. Xing-kui, and X. Xiu-ying, "Domain Patterns and Phase Transitions in Ferroelectric Crystal $KNbO_3$," Chin. Phys. Lett. 13, 621 (1996).
21. M.M. Shamim and T. Ishidate, "Anomalous mode coupling and phase transition of $KNbO_3$ under high pressure," Solid State Comm. 113, 713 (2000).
22. Y. Furukawa, K. Kitamura, A. Alexandrovski, R. K. Route, M. M. Fejer, and G. Foulon, "Green induced absorption in MgO doped $LiNbO_3$," Appl. Phys. Lett. 78, 1970 (2001).
23. Judith R. Schwesyg, Matthias Falk, Chris R. Phillips, Dieter H. Jundt, Karsten Buse, and Martin M. Fejer, "Pyroelectrically induced photorefractive damage in magnesium-doped lithium niobate crystals," J. Opt. Soc. Am. B **28**, 1973-1987 (2011).
24. A. Ashkin, G. D. Boyd, J. M. Dziedzic, R. G. Smith, A. A. Ballman, A. A. Levinstein, and K. Nassau, "Optically-Induced Refractive Index Inhomogeneities in LiNbO3 and LiTaO3," Appl. Phys. Lett **9**, 72 (1966).
25. B. E. Schmidt, N. Thire, M. Boivin, A. Laramée, F. Poitras, G. Lebrun, T. Ozaki, H. Ibrahim, and F. Légaré, "Frequency domain optical parametric amplification," Nature Communications 5, 3643 (2014).

OCIS Codes: 190.4400, 190.497, 140.3070